

## BIOMARKER CHARACTERIZATION OF VARIOUS OIL SHALE GRADES IN THE UPPER CRETACEOUS QINGSHANKOU FORMATION, SOUTHEASTERN SONGLIAO BASIN, NE CHINA

FEI HU<sup>(a,b)\*</sup>, ZHAOJUN LIU<sup>(a,b)</sup>, QINGTAO MENG<sup>(a,b)</sup>,  
JIANPENG WANG<sup>(c)</sup>, QINGLEI SONG<sup>(a,b)</sup>,  
WENQUAN XIE<sup>(a,b)</sup>

<sup>(a)</sup> College of Earth Sciences, Jilin University, 130061 Changchun, China

<sup>(b)</sup> Key Laboratory of Oil Shale and Coexistent Energy Minerals of Jilin Province, 130061 Changchun, China

<sup>(c)</sup> School of Earth and Environmental Sciences, University of Manchester, M13 9PL Manchester, UK

**Abstract.** *In the Songliao Basin, northeastern China, the oil shale-bearing succession in the Upper Cretaceous Qingshankou Formation contains excellent source rocks. Oil shales with different total organic carbon (TOC) contents and oil yields developed in the lower member of the formation ( $K_2qn^1$ ). In this study, we apply gas chromatography-mass spectrometry (GC-MS) to determine the geochemical characteristics, organic matter (OM) sources and depositional environments of various grades of oil shale. Rock-Eval pyrolysis indicates that type I kerogen is the predominant organic matter in the  $K_2qn^1$  oil shale, though variability in n-alkanes, steranes and hopanoids contents implies that organic matter from a variety of sources is present. High-quality oil shales are dominated by phytoplanktonic/algal and bacterial organic matter, while lower-quality oil shales are dominated by planktonic kerogen with a minor contribution from land plants. Organic matter types can indicate a high shale oil conversion rate, and increased prospects for oil shale utilization. Oxygen-deficient bottom water conditions, related to salinity stratification, are evidenced by biomarker ratios (Pr/Ph, gammacerane index (GI)). We propose that the highest-quality oil shales were deposited under anoxic conditions, with strong salinity stratification of the water column. OM sources, redox conditions and water column salinity stratification were the key factors controlling the accumulation of high-quality oil shale in the southeastern Songliao Basin.*

**Keywords:** *biomarker, high-quality oil shale, depositional environment, organic matter accumulation, alginite.*

---

\* Corresponding author: e-mail [hufei@jlu.edu.cn](mailto:hufei@jlu.edu.cn)

## 1. Introduction

The Songliao Basin is one of the largest Cretaceous continental basins in the world, and contains abundant oil and gas resources [1–4]. The Upper Cretaceous Qingshankou and Nenjiang formations are the most important source rocks [5], constituting 59% of total oil shale resources in China [6–7]. Previous studies have shown that the Songliao Basin contains mainly low- to medium-quality oil shale [6, 8]. However, new exploration has revealed the existence of oil shale layers with high total organic carbon (TOC) content (18.3–19.9 wt%) and oil yield (12.7–16.4 wt%) in the lowermost member of the Qingshankou Formation (K<sub>2</sub>qn<sup>1</sup>) [9], providing an exciting opportunity for oil shale development.

The Qingshankou Formation has attracted attention because of its excellent oil and gas production potential. Previous studies have mainly focused on this hydrocarbon potential [10, 11], as well as depositional environments [12–14], conditions of organic matter (OM) accumulation [5, 15–18], and oil shale resource evaluation [6, 19]. Biomarkers such as hopanes and steranes have received some attention, due to their usefulness as indicators of organic matter type and quality, depositional conditions (e.g. salinity, redox conditions, etc.), OM maturity level and the extent of biodegradation [20–22]. However, a detailed study of environmental change and the evolution of OM sources during the deposition of oil shales of different qualities is not yet available.

The aim of this study is to compare the geochemical characteristics of different grades of oil shale in the southeastern Songliao Basin, to shed light on salinity, redox conditions, and the sources of organic matter during oil shale deposition. This study will improve our understanding of the key factors controlling the formation of oil shales of different qualities, and determine next steps for oil shale exploration in the Songliao Basin.

## 2. Geological setting

The Songliao Basin is located in northeastern China with an area of approximately 260,000 km<sup>2</sup>. It is a Meso-Cenozoic composite sedimentary basin, with a dual fault-depression structure [5, 10, 17, 23]. Based on the basement geometry and the geological characteristics of the sedimentary succession, the Songliao Basin can be divided into six first-order structural units [1] (Fig. 1a). Oil shale is distributed mainly in the central depression, as well as the southeastern and northeastern uplift zones [17, 24].

The Songliao Basin contains an approximately 10-km-thick succession of Jurassic through Cenozoic siliciclastic deposits [1, 25]. Lower Cretaceous strata consist of the Huoshiling, Shahezi, Yingcheng, Denglouku and Quantou formations. The Upper Cretaceous is divided into the Qingshankou,

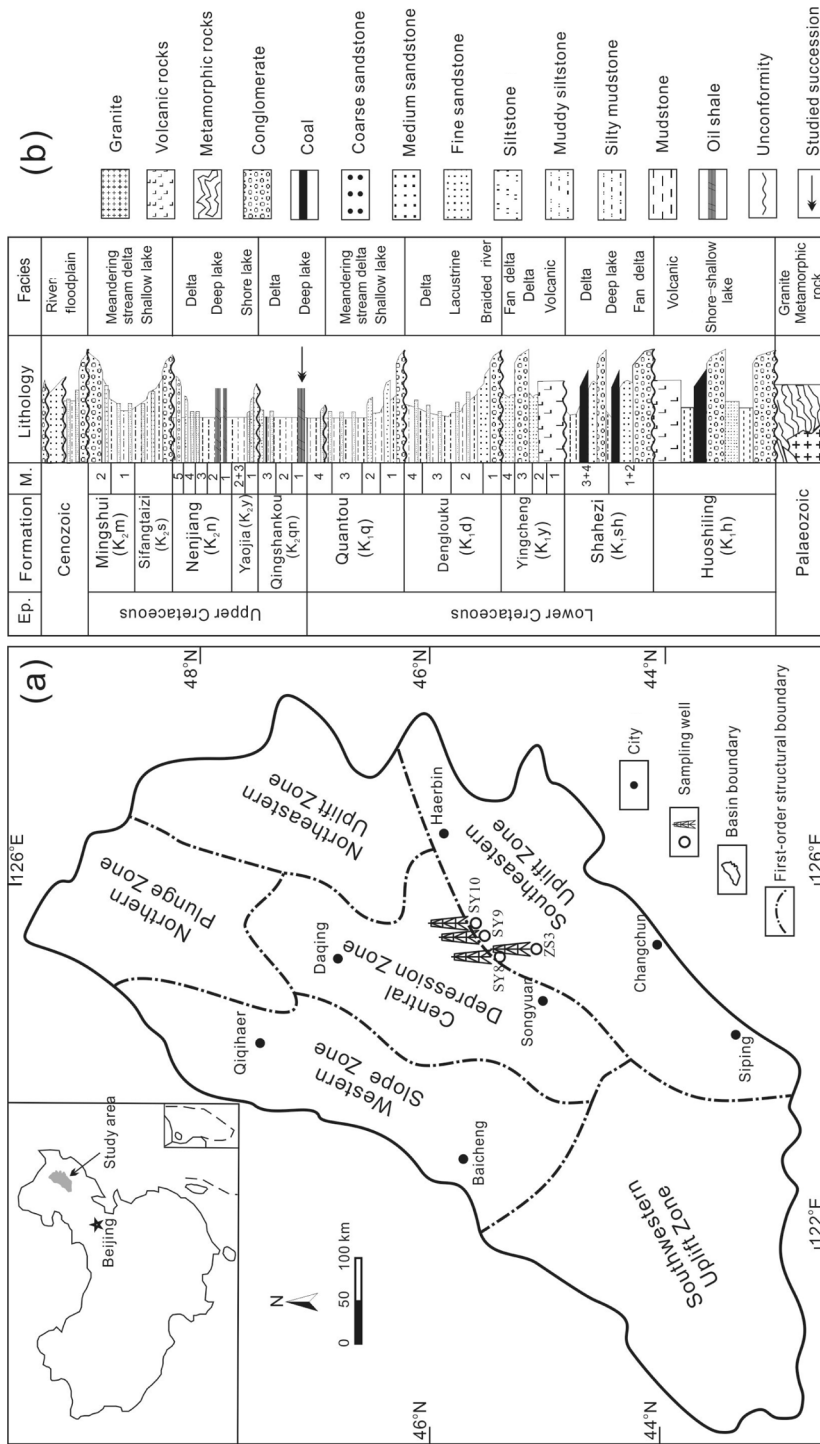


Fig. 1. Location map showing the Songliao Basin and its structural units. Generalized stratigraphic column is modified from [1]. (The abbreviations used: Ep. = epoch, M. = member.)

Yaojia, Nenjiang, Sifangtai and Mingshui formations, which are predominantly composed of terrigenous clastic rocks deposited in fluvial and lacustrine environments (Fig. 1b). A major target layer for hydrocarbon exploration is K<sub>2</sub>qn which is subdivided into three members, by lithology: K<sub>2</sub>qn<sup>1</sup>, K<sub>2</sub>qn<sup>2</sup> and K<sub>2</sub>qn<sup>3</sup>. The oil shale succession occurs in the lowermost member (K<sub>2</sub>qn<sup>1</sup>), which was deposited in a semi-deep to deep lake environment (Fig. 1b), and is composed of dark gray to gray-black mudstone, shale and oil shale [5, 9, 19].

### 3. Material and methods

A total of sixty-nine drill core samples were collected from the southeast uplift area of the Songliao Basin. Fifty-seven samples were collected at depths between 759.1 and 818.4 m from well ZS3; twelve more samples were collected at depths between 234.3 and 245.3 m from well SY9 (Fig. 1a). Each sample represented a composite of a 1-m-thick interval of core. All samples were analyzed for TOC (wt%), total sulfur (S, wt%), Fischer assay oil yield (FA, wt%), and Rock-Eval parameters. Based on these results, ten oil shale samples with different oil yields were selected for biomarker analysis. In addition, nine subsamples were selected from samples SY 8, SY 9 and SY 10 for petrographic analysis.

Each sample (< 250 μm) was pretreated with concentrated HCl to remove carbonate, allowing us to determine TOC and sulfur content on a Leco CS-230 elemental analyzer. Pyrolysis measurements were carried out using a Rock-Eval 6 instrument. The quantity of the pyrolyzate generated from kerogen during gradual heating in a helium stream was normalized to TOC, to give the hydrogen index ( $HI = S_2 \times 100/TOC$ , mg HC/g TOC). The temperature of maximum hydrocarbon generation ( $T_{max}$ ) served as an indicator of maturity. FA oil yield, determined by low temperature carbonization (about 520 °C) of 1-m-long core intervals, was measured using the Fischer assay method with a Chinese Fushun retort.

Soluble organic matter was extracted for biomarker analysis using a Soxhlet apparatus with chloroform eluent. The solvent extract was separated into saturate, aromatic and resin fractions with a silica gel:alumina (3:1) column after the precipitation of asphaltenes. The saturate fractions were analyzed using an Agilent 6890 gas chromatograph equipped with a fused silica column (30 m × 0.32 mm ID × 0.2 μm film). The oven was heated from 80 °C to 300 °C at a rate of 6 °C/min, and then held at 300 °C for 20 min. The injector was set at 310 °C in splitless mode, with hydrogen used as the carrier gas [26]. The gas chromatography-mass spectrometry (GC-MS) analysis (m/z 191, m/z 217, m/z 231) was performed using an Agilent 5973 N mass spectrometer with an HP-5MS fused silica column (30 m × 0.25 mm ID × 0.25 μm film). The injector temperature was 300 °C, and the emission current was 200 μA.

## 4. Results

### 4.1. Bulk geochemical parameters

Minimum, maximum and average values of oil yield, total organic carbon content, hydrogen index and temperature of maximum hydrocarbon generation from the  $K_2qn^1$  oil shale are reported in Table 1, and the stratigraphic distributions of these values are shown in Figure 2.

TOC content and oil yields vary significantly between oil shale layers, as well as between their floor and roof rocks (Fig. 2a–b, e–f). Oil yield from oil shales from different layers varies between 3.6 and 16.4 wt%, with an average value of 5.4 wt%, indicating that middle- to high-quality oil shale developed in  $K_2qn^1$ . Within the oil shale layers, TOC contents reach a maximum of 19.9 wt%, with the corresponding oil yield value reaching 16.4 wt% (layer 2; Fig. 2a–b). Cross-plots of TOC vs FA for all samples show a positive correlation ( $R^2 = 0.88$ ), which indicates that samples with a TOC content > 4.4 wt% can be considered oil shale (FA > 3.5 wt%; Fig. 3a). TOC contents of mudstones (1.8–6.4 wt%) in  $K_2qn^1$  are generally lower than those of oil shale layers, and the oil yields are consistently lower than 3.5 wt% (Table 1).

HI values in oil shale layers range from 620 to 1474 mg HC/g TOC (average 814 mg HC/g TOC); the maximum HI value is in layer 4 (Fig. 2c). Within mudstone layers, HI values are generally lower than those of oil shale

**Table 1. Minimum, maximum and average values of oil yield, TOC, sulfur, HI,  $T_{max}$  and TOC/S in different layers of oil shale and mudstone from  $K_2qn^1$**

Formation	Sample		Oil yield (FA), wt%		TOC, wt%		Sulfur, wt%	
			Min.–max.	Average	Min.–max.	Average	Min.–max.	Average
$K_2qn^1$	Oil shale	layer 6	–	5.1	–	6.6	–	1.0
		layer 5	3.6–4.6	4.1	4.4–5.7	5.1	0.9–1.2	1.0
		layer 4	3.6–5.4	4.5	2.6–6.2	4.1	0.6–1.1	0.9
		layer 3	3.6–6.7	5	3.9–7.3	5.5	0.9–4.1	1.7
		layer 2	3.6–16.4	6.5	3.4–19.9	8.1	0.9–2.4	1.7
		layer 1	4.7–7.0	5.8	6.5–7.3	6.9	1.4–1.7	1.5
	Mudstone	1.3–3.3	2.3	1.8–6.4	3.1	0.4–2.0	1.0	

Formation	Sample		HI, mg HC/g TOC		$T_{max}$ , °C		TOC/S	
			Min.–max.	Average	Min.–max.	Average	Min.–max.	Average
$K_2qn^1$	Oil shale	layer 6	–	757	–	442	–	7
		layer 5	782–783	782.5	443–446	445	3.7–6.5	5.1
		layer 4	755–1474	1053	447–449	448	3.2–8.2	4.9
		layer 3	757–845	799	443–449	446	0.9–6.0	4.3
		layer 2	620–818	742	441–448	445	2.9–11.2	4.6
		layer 1	727–769	748	439–445	442	3.8–5.2	4.5
	Mudstone	162–815	646	439–448	444	1.2–17.8	3.7	

Note: “–” represents no data.

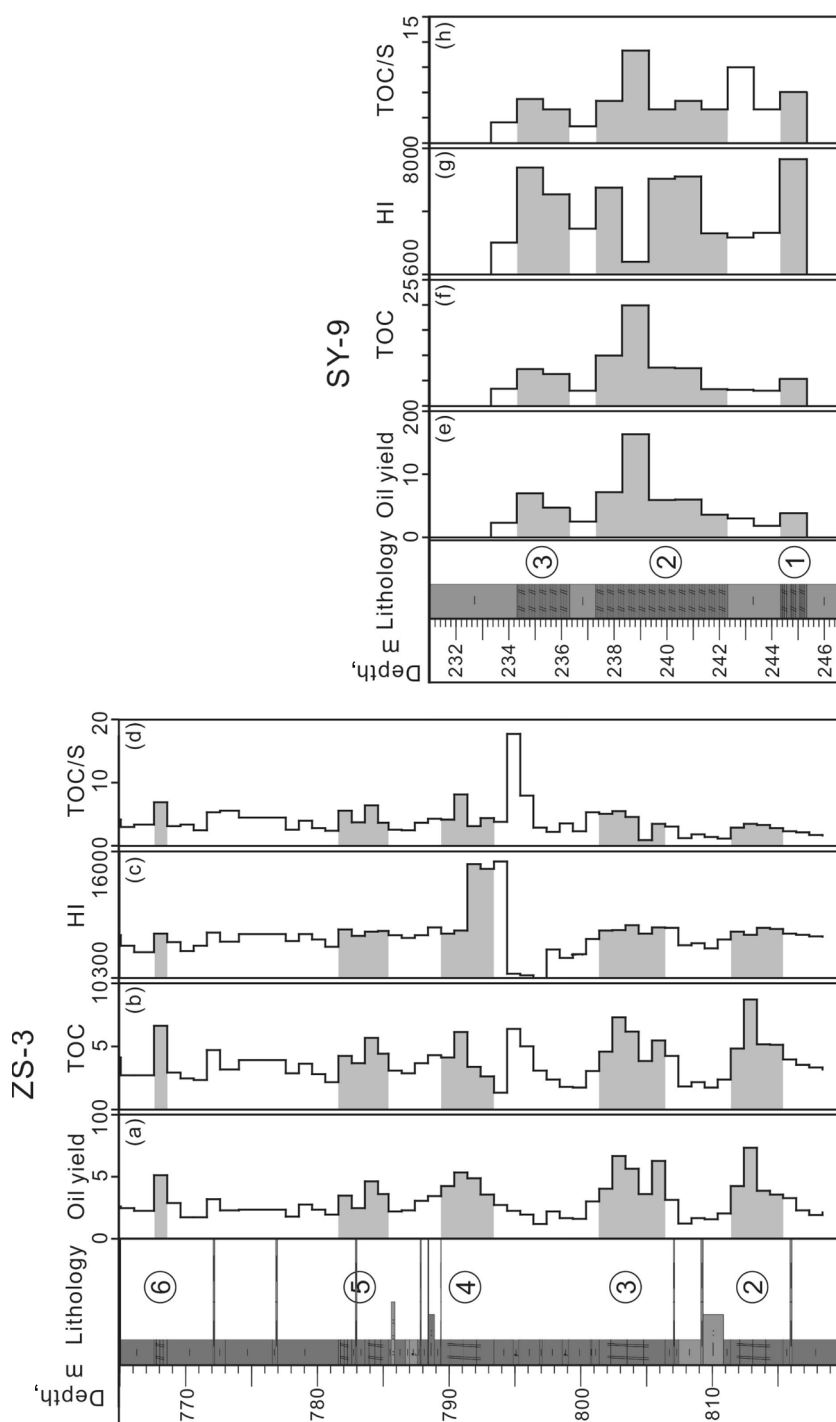


Fig. 2. Depth profiles of bulk geochemical proxies of oil shale and mudstones in K<sub>2</sub>qn<sup>1</sup>. Oil shale layers are numbered from bottom to top.

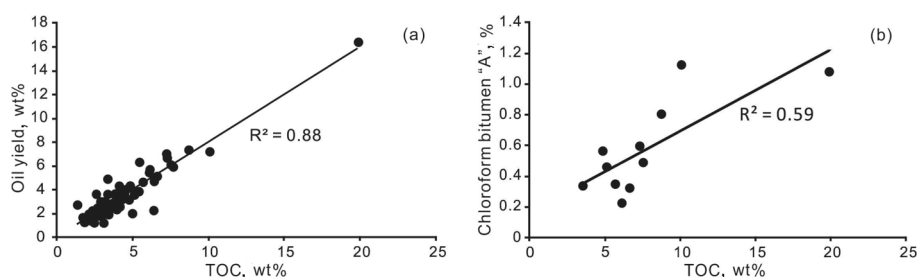


Fig. 3. Correlation between TOC and oil yield (a), and TOC and chloroform bitumen "A" (b) of samples from K<sub>2</sub>qn<sup>1</sup>.

layers, varying from 162 to 815 mg HC/g TOC, except for the 1-m-thick interval (793.4–794.4 m depth) in layer 4, with a maximum value of 1500 mg HC/g TOC (Fig. 2c). Most oil shale and mudstone samples plot inside the fields characteristic of type I kerogen (Fig. 4a–b), and only a few mudstone samples with type II kerogen are present (Fig. 4a, c).  $T_{\max}$  values vary between 439 and 449 °C, indicating that the samples are mostly of low thermal maturity. Sulfur content is low (0.4–2.0 wt%) in low-organic mud-

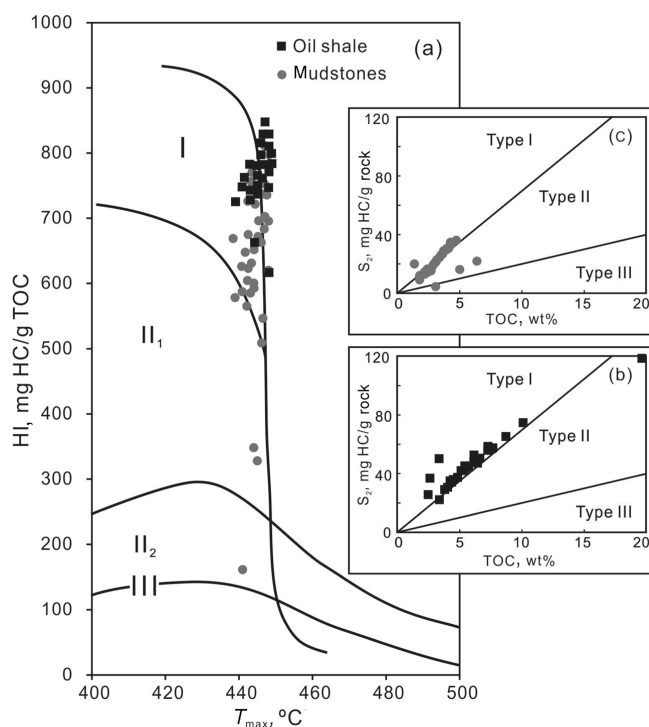


Fig. 4. (a) Plot of HI vs  $T_{\max}$  (according to [27]) outlining kerogen types of sediments from K<sub>2</sub>qn<sup>1</sup>; (b) plot of  $S_2$  vs TOC for oil shale; (c) plot of  $S_2$  vs TOC for mudstones (both according to [28]).

stones, but relatively high (0.6–4.1 wt%) in oil shale layers (Table 1). TOC/S ratios in most of the samples are also relatively low (< 10; Fig. 2d, h), with the highest TOC/S ratio occurring in the mudstone layer at a depth of 794.4–795.4 m (17.8; Fig. 2d). Within the oil shale layers, the highest TOC/S ratio occurs in those oil shales of layer 2 whose oil yields are the highest (11.2; Fig. 2d).

#### 4.2. Organic petrology and vitrinite reflectance

Nine oil shale and mudstone samples from  $K_2qn^1$  in the southeastern Songliao Basin were selected for maceral analysis. All samples were characterized by high sapropelitic content (95%; Table 2), and minor vitrinite and minor inertinite. Because the thin sections were processed using the kerogen enrichment method, amorphous sapropelic OM is the main maceral in the sapropelitic group. Bechtel et al. [5] proposed that organic matter in oil shale samples is dominated by lamalginite and telalginite. Type indices (TI) of all samples are greater than 80 (87–93; Table 2), indicating that oil shale and mudstone layers are composed of type I kerogen. Vitrinite reflectance was measured on six samples, and ranges from 0.5 to 0.66% (Table 2). These values are consistent with  $T_{max}$  data, and indicate that the oil shale and mudstone layers in  $K_2qn^1$  are immature to poorly mature.

**Table 2. Organic maceral and vitrinite reflectance of oil shale and mudstone samples from  $K_2qn^1$**

Bore-hole	Sample	Depth, m	Lithology	Oil yield, %	Sapropelic group (a), %	Liptinite (b1 + b2), %	Vitrinite (c), %	Inertinite (d), %	TI	Type of kerogen	Ro%
					Sapropelic amorphous		Collinite	Fusinite			
SY-10	SY-53	172.94	Oil shale	6.6	95.0	–	1.7	3.3	90	I	0.66
	SY-57	183.4		4.66	96.7	–	–	3.3	93	I	0.65
	SY-60	195.12		2.38	96.7	–	–	3.3	93	I	–
SY-8	SY-85	127.98	Mudstone	1.88	95.0	–	1.7	3.3	90	I	0.5
	SY-87	144.85		1.7	95.0	–	1.7	3.3	90	I	–
	SY-88	156.7		1.12	95.0	–	1.7	3.3	90	I	0.51
	SY-92	173.25		0.32	95.0	–	1.7	3.3	90	I	–
	SY-93	233.62		1.48	93.3	–	1.7	5.0	87	I	0.54
SY-9	SY-96	244.62	Oil shale	4.48	93.3	–	1.7	5.0	87	I	0.55

Note: “–” represents no data.

#### 4.3. Molecular composition of hydrocarbons

Within the studied oil shales, the chloroform bitumen “A” content ranges from 0.224 to 1.125 wt% (Table 3), and has a moderately positive correlation with TOC (Fig. 3b). The proportion of hydrocarbons in the oil shale

**Table 3. Bulk organic geochemical data about oil shales of different qualities from K<sub>2</sub>qn<sup>1</sup>**

Oil shale layer	Sample	Top depth, m	Bottom depth, m	Quality of oil shale	Oil yield, wt%	TOC, wt%	Chloroform bitumen "A" <sup>3a</sup> , wt%	Saturates, wt%, EOM	Aromatics, wt%, EOM	Resins, wt%, EOM	Asphaltenes, wt%, EOM
Layer 6	ZS3-9	767.60	768.60	Medium	5.14	6.64	0.32	49.39	11.63	36.24	2.74
Layer 5	ZS3-22	783.60	784.60	Poor	4.63	5.69	0.35	61.40	11.41	23.05	4.14
Layer 4	ZS3-29	790.40	791.40	Medium	5.38	6.15	0.22	63.72	18.74	15.73	1.81
Layer 3	ZS3-41	802.40	803.40	Medium	6.67	7.31	0.60	59.63	14.30	23.97	2.10
Layer 2	ZS3-50	811.40	812.40	Poor	4.27	4.86	0.56	49.23	10.95	31.59	8.22
	ZS3-51	812.40	813.40	Medium	7.34	8.73	0.80	55.54	15.53	24.71	4.22
	ZS3-53	814.40	815.40	Poor	3.59	5.14	0.46	55.72	15.18	24.10	5.00
	SY9-5	240.32	241.32	Medium	6.06	7.55	0.49	69.69	9.20	19.90	1.22
	SY9-7	238.32	239.32	High	16.37	19.90	1.08	55.10	17.68	26.43	0.80
	SY9-8	237.32	238.32	Medium	7.20	10.10	1.12	67.71	10.40	20.64	1.26

<sup>a</sup> Chloroform bitumen = mass percentage of extracted organic matter and samples; EOM – extracted organic matter.

layers is very high, ranging from 60 to 82%, indicating low-maturity OM, which is in agreement with Ro values of 0.5–0.66%. Saturated hydrocarbons (avg 59% of extracted organic matter (EOM)) dominate the aromatic fractions (avg 13% of EOM), which dominates the EOM pool. EOM also contains resins (avg 25% of EOM) and asphaltenes (avg 3% of EOM).

#### 4.3.1. Straight-chain alkanes

Total ion chromatograms (TIC) of saturated hydrocarbons of representative samples of different oil shale qualities are shown in Figure 5. The concentrations and ratios of compounds and compound groups in the various hydrocarbon fractions are given in Table 4.

Different distributions of *n*-alkanes are observed in different grades of oil shale. The high-quality oil shales (FA > 10%) display a high proportion of short-chain (*n*-C<sub>15–19</sub>) (avg 32%) and intermediate-chain (*n*-C<sub>21–25</sub>) (avg 32%) *n*-alkanes, with an odd-number predominance (CPI = 1.21; carbon preference index according to Bray and Evans [29]). The medium- (FA 5–10%) and poor-quality (FA 3.5–5%) oil shales are dominated by *n*-alkanes of intermediate (*n*-C<sub>21–25</sub>) (avg 35%) and long-chain (*n*-C<sub>27–31</sub>) length, with variable odd-number predominance (CPI 1.13–1.88) (Table 4). In comparison, the proportion of long-chain compounds in poor-quality oil shales (avg 24%) is slightly higher than in medium-quality oil shales (avg 21%).

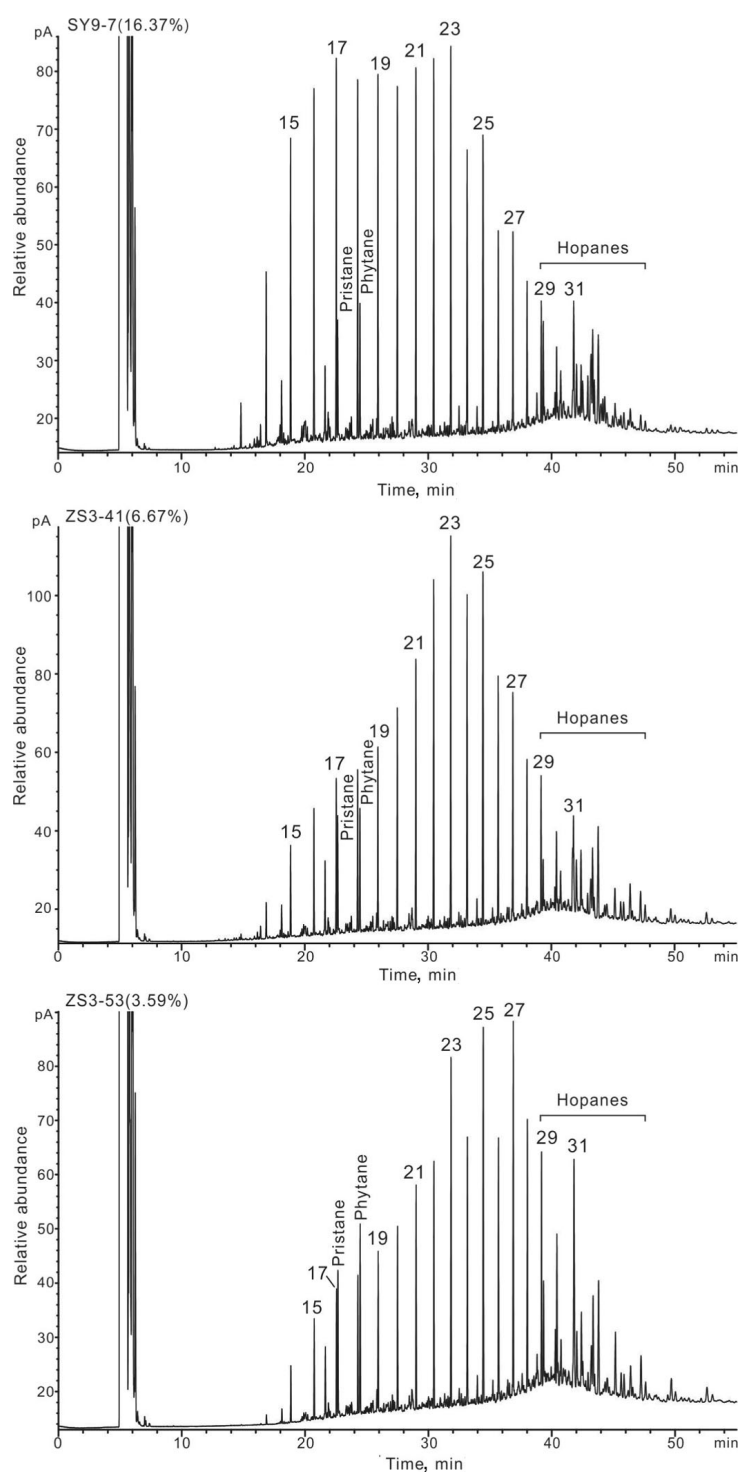


Fig. 5. Gas chromatograms (TICs) of saturated hydrocarbon fractions of different-quality oil shales. *n*-Alkanes are labeled according to their carbon number.

Table 4. Biomarker analysis data

Oil shale layer	Sample	Top depth, m	Bottom depth, m	Straight-chain alkanes				Acyclic isoprenoids		
				$n\text{-C}_{15}\text{-C}_{19}/n\text{-alk, \%}$	$n\text{-C}_{21}\text{-C}_{25}/n\text{-alk, \%}$	$n\text{-C}_{27}\text{-C}_{31}/n\text{-alk, \%}$	CPI <sup>a</sup>	Pr <sup>b</sup> /Ph <sup>c</sup>	Pr/nC <sub>17</sub>	Ph/nC <sub>18</sub>
Borehole ZS3										
Layer 6	ZS3-9	767.60	768.60	24.73	27.68	23.58	1.88	1.42	0.88	0.75
Layer 5	ZS3-22	783.60	784.60	19.55	30.92	20.71	1.24	0.87	0.99	1.13
Layer 4	ZS3-29	790.40	791.40	18.65	35.85	20.02	1.13	1.05	0.79	0.68
Layer 3	ZS3-41	802.40	803.40	13.56	38.39	25.17	1.19	0.80	0.57	0.61
Layer 2	ZS3-50	811.40	812.40	13.04	41.08	19.42	1.35	0.80	1.39	1.62
	ZS3-51	812.40	813.40	16.40	33.47	22.07	1.35	0.84	1.39	1.74
	ZS3-53	814.40	815.40	11.78	30.90	31.51	1.49	0.75	1.26	1.56
Borehole SY9										
Layer 2	SY9-5	240.32	241.32	16.33	41.03	18.92	1.23	0.94	0.87	0.88
	SY9-7	238.32	239.32	31.58	31.87	13.98	1.21	0.83	0.34	0.44
	SY9-8	237.32	238.32	26.95	33.25	17.58	1.20	0.74	0.40	0.54

	Sample	Top depth, m	Bottom depth, m	Sterane					Terpenoids				
				$5\alpha\text{-C}_{27}, \%$	$5\alpha\text{-C}_{28}, \%$	$5\alpha\text{-C}_{29}, \%$	$\Sigma(\text{C}_{27}+\text{C}_{28})/\Sigma\text{C}_{29}$	$\Sigma\text{C}_{27}/\Sigma\text{C}_{29}$	$\text{C}_{29}\alpha\alpha 20\text{S}/20(\text{R} + \text{S})$	Ts <sup>d</sup> /Tm <sup>e</sup>	$22\text{S}/(22\text{S} + 22\text{R})\text{C}_{31}$ hopanes	GI <sup>f</sup>	Moretane/17 $\alpha$ 21 $\beta$ C <sub>30</sub> hopane
Borehole ZS3													
Layer 6	ZS3-9	767.60	768.60	38.01	25.77	36.22	1.76	1.05	0.15	0.47	0.47	0.18	0.15
Layer 5	ZS3-22	783.60	784.60	32.31	27.22	40.47	1.47	0.80	0.13	0.51	0.51	0.28	0.15
Layer 4	ZS3-29	790.40	791.40	25.57	30.46	43.98	1.27	0.58	0.20	0.50	0.50	0.24	0.16
Layer 3	ZS3-41	802.40	803.40	26.81	31.51	41.68	1.40	0.64	0.14	0.50	0.50	0.66	0.20
Layer 2	ZS3-50	811.40	812.40	37.80	27.80	34.40	1.91	1.10	0.16	0.52	0.52	0.65	0.19
	ZS3-51	812.40	813.40	45.42	24.67	29.91	2.34	1.52	0.19	0.51	0.51	0.45	0.18
	ZS3-53	814.40	815.40	52.19	14.80	33.01	2.03	1.58	0.18	0.51	0.51	0.52	0.19
Borehole SY9													
Layer 2	SY9-5	240.32	241.32	44.87	23.53	31.59	2.17	1.42	0.14	0.51	51	0.38	0.16
	SY9-7	238.32	239.32	42.93	26.23	30.84	2.24	1.39	0.13	0.43	43	0.63	0.20
	SY9-8	237.32	238.32	46.82	24.96	28.22	2.54	1.66	0.14	0.41	41	0.39	0.20

<sup>a</sup> Carbon preference index (according to [27])

<sup>b</sup> Pristane

<sup>c</sup> Phytane

<sup>d</sup> 17 $\alpha$ C<sub>27</sub> Hopane

<sup>e</sup> 17 $\beta$ C<sub>27</sub> Hopane

<sup>f</sup> Gammacerane index

The abbreviation used: alk – alkanes.

Generally, the low molecular weight *n*-alkanes are found in algae and microorganisms [30]. Alkanes of intermediate molecular weight have been reported to originate from sphagnum or aquatic macrophytes [31]. Long-chain alkanes are characteristic biomarkers for terrestrial plants, as they are the main components of leaf waxes [32]. The *n*-alkane distribution in  $K_2n^1$  oil shale may reflect the primary role of algae and aquatic macrophytes in OM contribution to high-quality oil shale formation, and the role of aquatic macrophytes and land plants in OM contribution to the formation of medium- and poor-quality oil shales.

#### 4.3.2. Acyclic isoprenoids

The isoprenoids pristane (Pr) and phytane (Ph) are abundant in all oil shale samples (Fig. 5). The Pr/Ph ratio has been used extensively as an indicator of redox conditions in the depositional environment [33], though it may also be affected by maturation [20], and by differences in the precursors of acyclic isoprenoids (e.g., bacterial origin [34, 35]). Generally, Pr/Ph ratios < 1.0 suggest anaerobic conditions during early diagenesis; values between 1.0 and 3.0 suggest dysaerobic conditions. The influence of different organic matter sources on Pr/Ph ratios in the present study can be ruled out, as most oil shale samples are dominated by phytane. The Pr/Ph ratio of high-quality oil shale is 0.83. The Pr/Ph ratio in the poor- and medium-quality oil shales ranges from 0.75 to 0.87 (avg 0.81) and from 0.74 to 1.42 (avg 0.97), respectively (Table 4). These data suggest that oil shales were deposited under anoxic to dysoxic conditions, this interpretation being supported by cross plotting Pr/*n*-C<sub>17</sub> vs Ph/*n*-C<sub>18</sub> (Fig. 6, [36]).

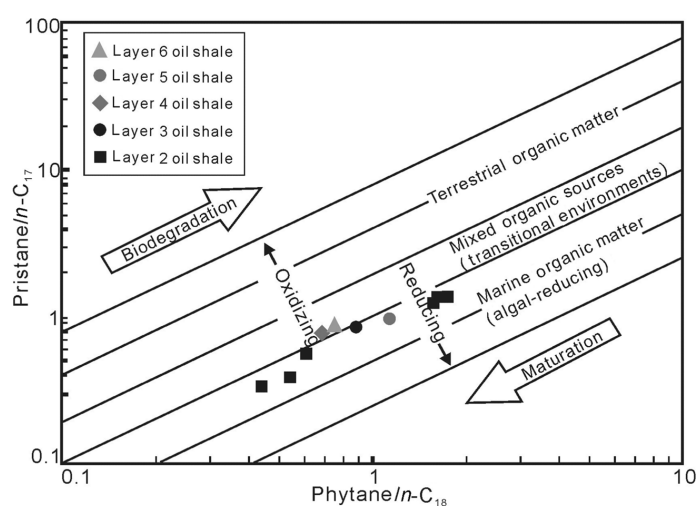


Fig. 6. Cross-correlation of pristane/*n*-C<sub>17</sub> vs phytane/*n*-C<sub>18</sub> for  $K_2qn^1$  oil shale.

### 4.3.3. Steroids

Steroids are abundant in all oil shale samples from the southeastern Songliao Basin. Based on  $m/z$  217 chromatograms (Fig. 7),  $5\alpha$ ,  $14\alpha$  and  $17\alpha(H)$  steranes are present in the  $C_{27}$ – $C_{29}$  range. They are dominated by the  $5\alpha$ ,  $14\beta$ , and  $17\beta(H)$  isomers, which is consistent with the low maturity of the samples. Diasteranes and pregnane are also present in low abundances.

The carbon number distributions of regular steranes ( $C_{27}$ – $C_{29}$ ) in different oil shale layers show different characteristics; the carbon number distribution is  $C_{27} > C_{29} > C_{28}$  (normal “L”-type) in layer 2 oil shales, and is dominated by  $C_{27}$  steranes (Fig. 7a–b). The carbon number distribution is  $C_{29} > C_{27} > C_{28}$  (reverse “L”-type) in layer 3 and 4 oil shales, which are dominated by  $C_{29}$  steranes (Fig. 7c–d). The distribution of regular steranes is  $C_{29} \approx C_{27} > C_{28}$  or  $C_{27} > C_{29} > C_{28}$  (“V”-type) in oil shales from layers 5 and 6 (Fig. 7e–f). Algae have been proposed to be the leading primary producer of  $C_{27}$  sterols, while land plants are associated with  $C_{29}$  sterols [37]. In contrast,  $C_{28}$  steranes are believed to have been derived from a variety of sources [38–41]. Based on a ternary diagram plotting the relative proportions of  $C_{27}$ ,  $C_{28}$  and  $C_{29}$  steranes (Fig. 8), we suggest that algal and mixed planktonic-

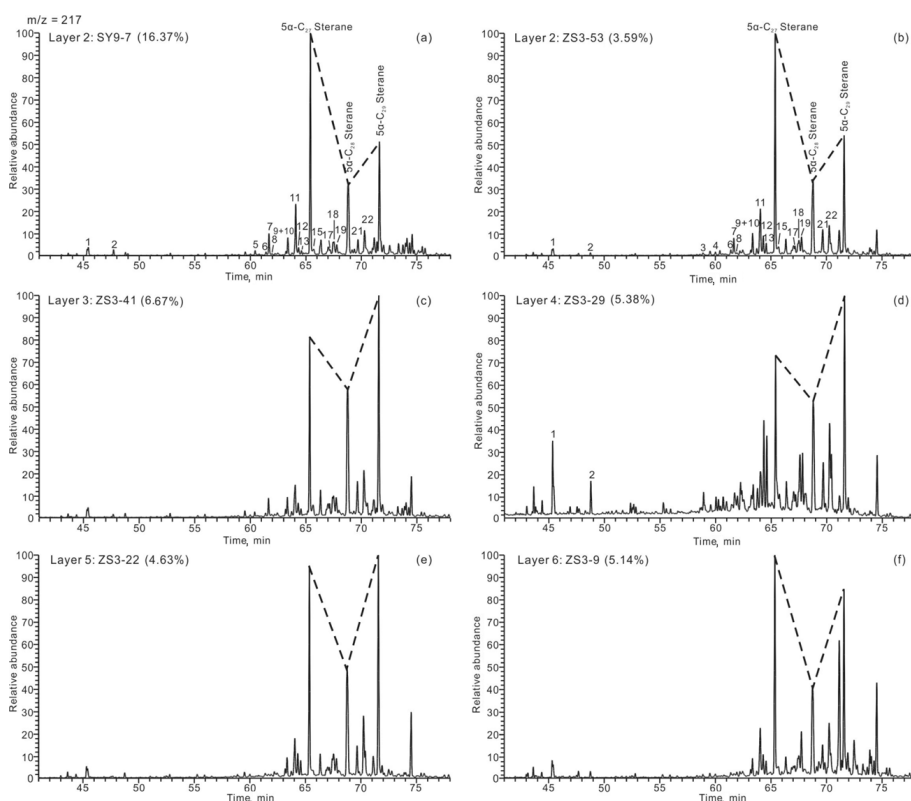


Fig. 7. Mass chromatograms ( $m/z$  217) for steranes of oil shale from different layers of  $K_2qn^1$ .

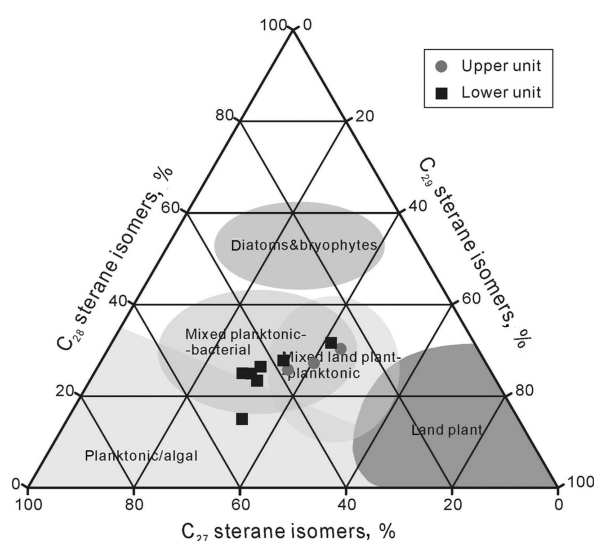


Fig. 8. Ternary diagram of the composition of  $C_{27}$ ,  $C_{28}$  and  $C_{29}$  steranes, indicating different origins of organic matter. Discriminatory areas are from [42].

bacterial OM sources dominate the lower oil shale layers (layers 1 to 3), whereas mixed plankton and land plant sources dominate the upper oil shale layers (layers 4 to 6).

High concentrations of  $C_{28}$ ,  $C_{29}$  and  $C_{30}$  4-methylsteranes are detected in all oil shale samples; however, the 4-methylsterane content is variable between oil shale layers. This is indicative of different organic matter sources. 4-methylsteranes are more abundant in the lower oil shale unit than in the upper oil shale unit. The lower unit is dominated by  $C_{29}$  and  $C_{30}$  4-methylsteranes, whereas the upper unit is dominated by  $C_{29}$  4-methylsteranes. Within layer 2, high-quality oil shales have a higher 4-methylsterane content compared to lower-quality oil shales.

#### 4.3.4. Terpenoids

Terpenoids are the most widely distributed biomarker compounds in the sediment. Chromatograms ( $m/z$  191; Fig. 9) show that terpenoids, including pentacyclitriterpanes, tricyclic terpanes, gammacerane, and a small quantity of tetracyclic terpanes, are detected in all oil shale samples. Hopanoids are important non-aromatic cyclic triterpenoid constituents of oil shale in the southeastern Songliao Basin. The hopanoid distribution is characterized by  $17\alpha$ ,  $21\beta$  and  $17\beta$ ,  $21\alpha$  hopanes from  $C_{27}$  to  $C_{35}$ , with no  $C_{28}$  hopanes present. The predominant hopanoid is  $17\alpha$ ,  $21\beta$   $C_{30}$  hopane;  $C_{35}$  hopanes are not detected in layers 5 and 6.  $C_{31}$ - $C_{35}$  homohopanes gradually decrease in abundance with increasing carbon number as follows:  $C_{31} > C_{32} > C_{33} > C_{34} > C_{35}$ .

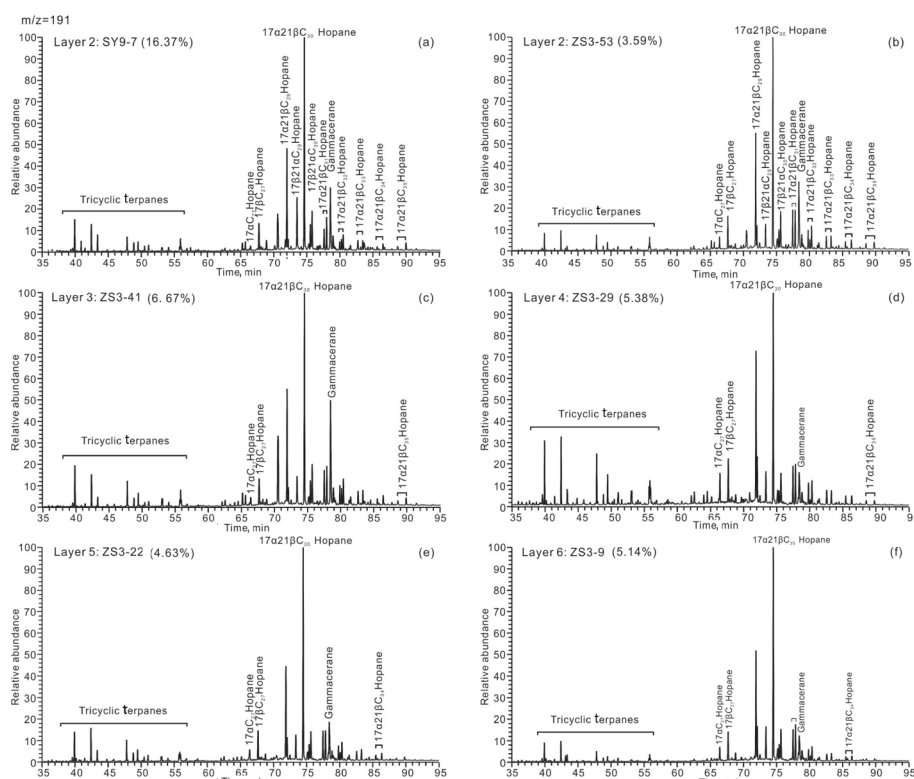


Fig. 9. Mass chromatograms ( $m/z$  191) for terpenoids of oil shale from different layers of  $K_2qn^1$ .

The ratio of the 22S to 22S + 22R isomers of  $17\alpha$ ,  $21\beta(H)$ - $C_{31}$  hopanes in the studied oil shale samples ranges from 0.41 and 0.52, lower than the end member value of 0.6 [43]. The ratio of  $\beta\alpha hC_{30}$  hopane (moretane) to  $\alpha\beta tC_{30}$  hopane ranges from 0.15 to 0.20 (Table 4), with little variability between the samples.

#### 4.3.5. Indicators of paleosalinity (gammacerane)

The abundance of gammacerane is often associated with OM deposition in hypersaline environments [44] and may record input from bacterivorous ciliates living at or below the chemocline in stratified lakes [45]. Gammacerane is present in variable amounts in all oil shale layers. The gammacerane index ( $GI = \text{gammacerane} / (\text{gammacerane} + \alpha\beta\text{-}C_{30} \text{ hopane})$ ) is a good indicator of salinity stratification of the water column in many lacustrine and marine sediments [22, 45, 46]. The GI values of oil shales in the Songliao Basin range from 0.18 to 0.66, and show a negative relationship with the Pr/Ph ratio (Fig. 10). The observed upward decrease in GI, which is accompanied by an upward increase in Pr/Ph ratios (Fig. 11c–d), indicates variable water column stratification associated with changes in salinity.

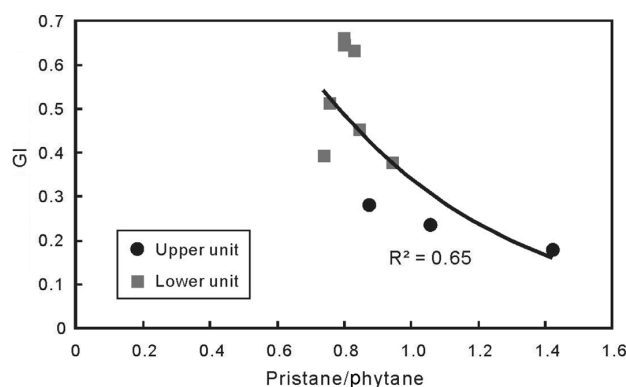


Fig. 10. Relationship between GI and pristane/phytane ratio of  $K_2qn^1$  oil shale.

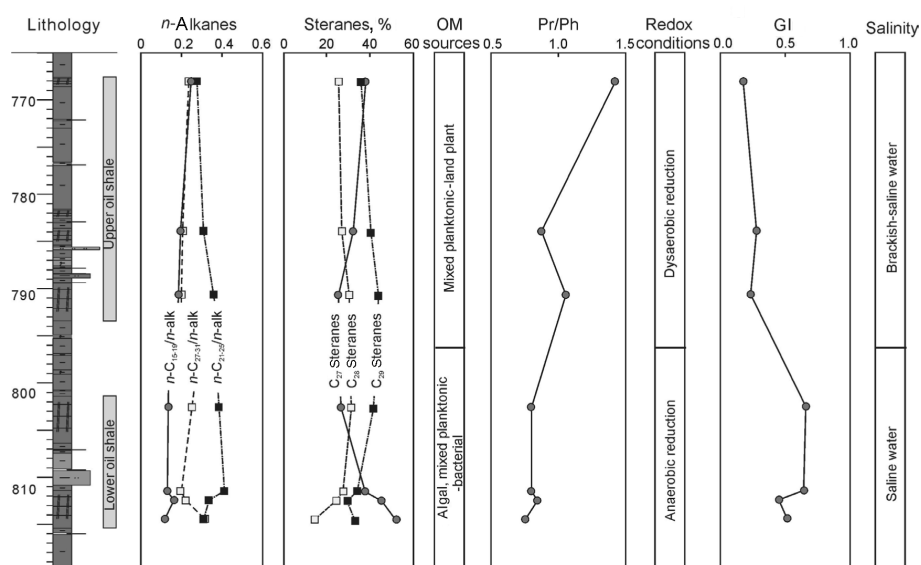


Fig. 11. Vertical evolution of  $n$ -alkanes, steranes, Pr/Ph and GI of  $K_2qn$  oil shale of the southeastern Songliao Basin. (The abbreviation used: alk – alkanes.)

## 5. Discussion

### 5.1. Hydrocarbon potential and oil shale quality

Upper Cretaceous lacustrine sediments are widespread in the Songliao Basin, especially in the Qingshankou Formation (Member 1;  $K_2qn^1$ ). Figure 12 shows the hydrocarbon generation potential of  $K_2qn^1$  source rocks in the southeastern Songliao Basin. All oil shale and mudstone samples that contain type I–II kerogen plot in the good to very good source rock region, indicating excellent hydrocarbon potential. Although the maturity of the

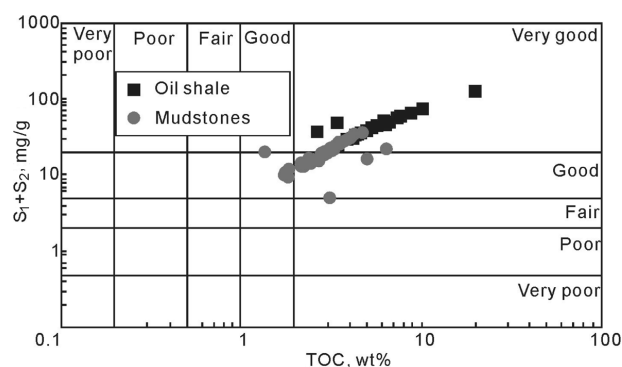


Fig. 12. Plot of  $S_1 + S_2$  vs TOC of  $K_2qn^1$  oil shale and mudstones (according to [47]).

studied samples (immature to marginally mature) is not high enough to generate and expel large amounts of hydrocarbons, thousands of productive wells from Daqing and Jilin Oil Field of PetroChina Company Limited confirm that oil is abundant in the central depression where the source rocks are of higher maturity.

The oil shales located in the southeastern uplift area of the Songliao Basin were not buried deep, and contain a large amount of immature OM. According to Meng et al. [8] and Liu et al. [7], the industrial grade of oil shale is of medium quality, with medium to high ash yields and low gross calorific values. Compared with the Huadian oil shale in northeastern China (3.6–19.8 wt%; avg 7.0 wt%) [15, 48], the oil yield of Songliao oil shale is relatively low (3.6–16.4 wt%; avg 5.4 wt%). However, the Songliao oil shale has a high shale oil conversion rate (oil yield/TOC ratio 0.7–1.5), while the Huadian oil shale has a low oil conversion rate, 0.3–0.7. The difference in oil yield and shale oil conversion rate may be related to the abundance and type of organic matter.

The relatively low oil yield of Songliao oil shale may be the result of low organic matter content in the very large Songliao lake basin, compared to the small, coal-bearing Huadian lake basin. The Songliao Basin is a large depression, covering an area of  $26 \times 10^4$  km<sup>2</sup>, and the organic matter is represented by lamalginite algae, plankton and bacteria (kerogen type I; Fig. 4b). In contrast, the Huadian Basin is a small, elongated, fault-controlled basin covering an area of 26 km<sup>2</sup>, and the organic matter represents various kerogen types (II<sub>1</sub>, II<sub>2</sub> and III) [15, 48]. The type I kerogen and high shale oil conversion rate of Songliao oil shale indicate that the type of OM is suitable for oil conversion and oil shale utilization.

## 5.2. Depositional environments and their implications for oil shale formation

The upper and lower oil shale units both accumulated in a relatively deep lacustrine environment. Geochemical and biomarker data from oil shale

layers are summarized in Figures 2 and 11. Changes in HI, *n*-alkanes and steranes in oil shale samples indicate that organic matter from different sources is present in different oil shale layers. Furthermore, the salinity and redox conditions can be evaluated based on the Pr/Ph ratio and gammacerane index. Differences in OM sources and environmental conditions (i.e. water column stratification and redox) may have controlled the quality and thickness of oil shales within the Qingshankou Formation.

### 5.2.1. Lower oil shale units (layers 1–3)

The oil shale units of deeper burial in the basin are characterized by a high TOC content (3.4–19.9 wt%) and medium to high oil yield (3.6–16.4 wt%) (Fig. 2a–b, e–f). Oil shale layers 1–3 are relatively thick and have moderate HI values (620–845 mg HC/g TOC; Fig. 2c, g). Maceral and biomarker data show that the OM pool is dominated by algal, planktonic and bacterial OM (Fig. 8; Fig. 11a–b). Terrestrial organic matter is abundant only in oil shale layer 3, resulting in a low oil yield (Fig. 7c). Low TOC/S ratios and high GI values, associated with low Pr/Ph values, indicate a stratified water column and saline, anoxic conditions in the bottom water (Fig. 13a).

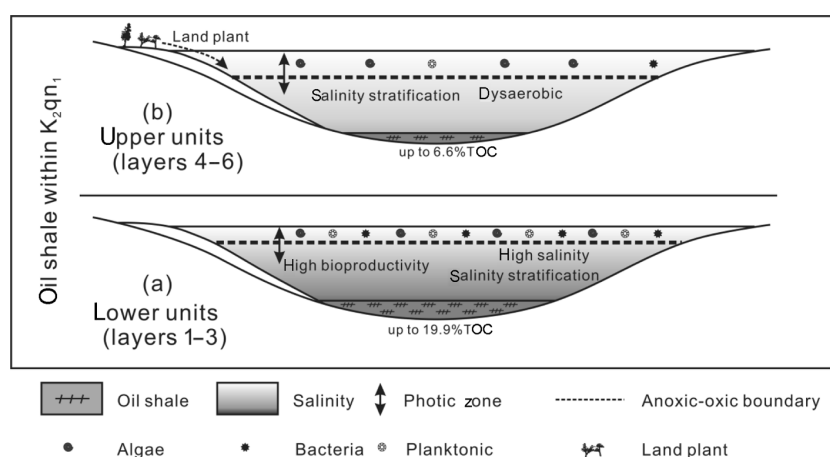


Fig. 13. Picture illustrating lower and upper oil shale units of the southeastern Songliao Basin (with no scale).

### 5.2.2. Upper oil shale units (layers 4–6)

Oil shale layers 4–6 are thin and are characterized by a moderate TOC content (2.6–6.6 wt%), low to medium oil yield (3.6–5.4 wt%) (Fig. 2 a–b), and very high HI values (755–1474 mg HC/g TOC) (Fig. 2c). High concentrations of land plant-derived biomarkers attest to a significant component of terrestrial organic matter in layers 4 and 5, which likely explains the low oil yield from those layers. The percentage of terrestrial and planktonic

organic matter gradually decreases from layer 4 to 6, while the percentage of algal material increases (Fig. 12a–b; Fig. 3b). Low TOC/S ratios and gammacerane index values also indicate water column salinity stratification, albeit to a lesser degree than in the lower oil shale units (Fig. 2d; Fig. 11d). High Pr/Ph values (0.87–1.42) suggest the bottom water was dyserobic (Fig. 11c).

## 6. Conclusions

1. Based on total organic carbon and Rock-Eval pyrolysis data, the oil shales and organic-rich mudstones of the Upper Cretaceous Qingshankou Formation in the southeastern Songliao Basin are excellent source rocks for oil, containing type I, immature to low-maturity organic matter.
2. The high organic matter content of the Songliao K<sub>2</sub>qn<sup>1</sup> oil shale controls the high shale oil conversion rate, and points toward potential success in the development and utilization of Songliao oil shale.
3. Changes in *n*-alkanes, steranes and hopanoids in K<sub>2</sub>qn<sup>1</sup> oil shale indicate that organic matter from various sources is present in the oil shales of different qualities. High-quality oil shale is dominated by phytoplanktonic/algal and bacterial organic matter, whereas low-quality oil shale is dominated from planktonic organic matter with a minor contribution from land plants.
4. Oxygen-deficient bottom water conditions, related to salinity stratification, are evidenced by biomarker data in certain oil shale layers. We propose that strong salinity stratification of the water column and persistent anoxic conditions accompanied the deposition of high-quality oil shale.
5. Over the scale of the southeastern Songliao Basin, the origin of organic matter and the depositional redox conditions and water salinity were the key factors controlling the quality and thickness of oil shales. Algal and microbial-derived organic matter, strong salinity stratification and anoxic conditions promoted the accumulation of high-quality oil shale.

## Acknowledgments

We would like to thank Mr. Junlin He, Senior Engineer in the Jilin Oil Field of PetroChina Company Limited, for providing access to core material. This study was supported by the Jilin Oil Field of PetroChina Company Limited (JLYT-JS13-W23-FW-11-79).

## REFERENCES

1. Feng, Z. Q., Jia, C. Z., Xie, X. N., Cross, T. A. Tectonostratigraphic units and stratigraphic sequences of the nonmarine Songliao basin, northeast China. *Basin Res.*, 2010, **22**(1), 79–95.
2. Liu, Z. J., Sun, P. C., Jia, J. L., Meng, Q. T., Rong, L. Distinguishing features and their genetic interpretation of stratigraphic sequences in continental deep water setting: a case from Qingshankou Formation in Songliao Basin. *Earth Sci. Front.*, 2011, **18**(4), 171–180.
3. Ren, Y. G., Zhu, D. F., Wan, C. B., Wang, C. Natural gas accumulation rule of Xujiaweizi depression in Songliao basin and future exploration target. *Pet. Geol. Oilfield Dev. Daqing*, 2004, **23**(5), 26–29 (in Chinese with English abstract).
4. Wu, F. Y., Sun, D. Y., Li, H. M., Wang, X. L. The nature of basement beneath the Songliao Basin in NE China: geochemical and isotopic constraints. *Phys. Chem. Earth A: Solid Earth Geod.*, 2001, **26**(9–10), 793–803.
5. Bechtel, A., Jia, J. L., Strobl, S. A. I., Sachsenhofer, R. F., Liu, Z., Gratzner, R., Püttmann, W. Palaeoenvironmental conditions during deposition of the Upper Cretaceous oil shale sequences in the Songliao Basin (NE China): implications from geochemical analysis. *Org. Geochem.*, 2012, **46**, 76–95.
6. Liu, Z. J., Yang, H. L., Dong, Q. S., Zhu, J. W., Guo, W., Ye, S. Q., Liu, R., Meng, Q. T., Zhang, H. L., Gan, S. C. *Oil Shale in China*. Petroleum Industry Press, Beijing, 2009, 157–167 (in Chinese with English abstract).
7. Liu, Z. J., Meng, Q. T., Dong, Q. S., Zhu, J. W., Guo, W., Ye, S. Q., Liu, R., Jia, J. L. Characteristics and resource potential of oil shale in China. *Oil Shale*, 2017, **34**(1), 15–41.
8. Meng, Q. T., Liu, Z. J., Liu, R., Wang, Y. L. Controlling factors on the oil yield of the Upper Cretaceous oil shale in the Nongan Area, Songliao basin. *Journal of Jilin University (Earth Science Edition)*, 2006, **36**(6), 963–968 (in Chinese with English abstract).
9. Xu, J. J., Liu, Z. J., Bechtel, A., Meng, Q. T., Sun, P. C., Jia, J. L., Cheng, L. J., Song, Y. Basin evolution and oil shale deposition during Upper Cretaceous in the Songliao Basin (NE China): Implications from sequence stratigraphy and geochemistry. *Int. J. Coal Geol.*, 2015, **149**, 9–23.
10. Gao, R. Q., Cai, X. Y. *The Forming Condition and Distribution Regularity of the Oil and Gas Fields in Songliao Basin*. Petroleum Industry Press, Beijing, 1997, 104–106 (in Chinese).
11. Zhou, Y., Littke, R. Numerical simulation of the thermal maturation, oil generation and migration in the Songliao Basin, Northeastern China. *Mar. Petrol. Geol.*, 1999, **16**(8), 771–792.
12. Feng, Z. H., Fang, W., Wang, X., Huang, C. Y., Huo, Q. L., Zhang, J. H., Huang, Q. H., Zhang, L. Microfossils and molecular records in oil shales of the Songliao Basin and implications for paleo-depositional environment. *Sci. China Ser. D-Earth Sci.*, 2009, **52**(10), 1559–1571.
13. Hou, D. J., Li, M. W., Huang, Q. H. Marine transgression events in the gigantic freshwater lake Songliao: paleontological and geochemical evidence. *Org. Geochem.*, 2000, **31**(7–8), 763–768.
14. Huang, Q., Chen, C., Wang, P., Han, M., Li, X., Wu, D. The late Cretaceous bio-evolution and anoxic events in the ancient lake in the Songliao Basin. *Acta Micropalaeontol. Sin.*, 1997, **15**(4), 417–425.

15. Sun, P. C., Sachsenhofer, R. F., Liu, Z. J., Strobl, S. A. I., Meng, Q. T., Liu, R., Zhen, Z. Organic matter accumulation in the oil shale-and coal-bearing Huadian Basin (Eocene; NE China). *Int. J. Coal Geol.*, 2013, **105**, 1–15.
16. Sun, P. C. *Environmental Dynamics of Organic Accumulation in the Oil Shale Bearing Layers in the Upper Cretaceous, Southeast Songliao Basin (NE China)*. PhD Thesis, Jilin University, 2013.
17. Jia, J. L., Liu, Z. J., Bechtel, A., Strobl, S. A. I., Sun, P. C. Tectonic and climate control of oil shale deposition in the Upper Cretaceous Qingshankou Formation (Songliao Basin, NE China). *Int. J. Earth Sci.*, 2013, **102**(6), 1717–1734.
18. Xu, J. J., Bechtel, A., Sachsenhofer, R. F., Liu, Z. J., Gratzner, R., Meng, Q. T., Song, Y. High resolution geochemical analysis of organic matter accumulation in the Qingshankou Formation, Upper Cretaceous, Songliao Basin (NE China). *Int. J. Coal Geol.*, 2015, **141–142**, 23–32.
19. Jia, J. L. *Research on the Recognition and Resource Evaluation of the Upper Cretaceous Oil Shale Based on Geochemistry-Geophysics Technique in the Songliao Basin (NE, China)*. PhD Thesis, Jilin University, 2012.
20. Tissot, B. T., Welte, D. H. *Petroleum Formation and Occurrence*. Second Revised and Enlarged Edition, Springer-Verlag, Berlin, 1984.
21. Moldowan, J. M., Sundararaman, P., Schoell, M. Sensitivity of biomarker properties to depositional environment and/or source input in the Lower Toarcian of SW-Germany. *Org. Geochem.*, 1986, **10**(4–6), 915–926.
22. Peters, K. E., Walters, C. C., Moldowan, J. M. *The Biomarker Guide. Volume 1: Biomarkers and Isotopes in the Environment and Human History. Volume 2: Biomarkers and Isotopes in Petroleum Exploration and Earth History*. Second Edition, Cambridge University Press, New York, NY, 2005.
23. Mi, J. K., Zhang, S. C., Hu, G. Y., He, K. Geochemistry of coal-measure source rocks and natural gases in deep formations in Songliao Basin, NE China. *Int. J. Coal Geol.*, 2010, **84**(3–4), 276–285.
24. Jia, J. L., Bechtel, A., Liu, Z. J., Strobl, S. A. I., Sun, P. C., Sachsenhofer, R. F. Oil shale formation in the Upper Cretaceous Nenjiang Formation of the Songliao Basin (NE China): Implications from organic and inorganic geochemical analyses. *Int. J. Coal Geol.*, 2013, **113**, 11–26.
25. Li, S. Q., Chen, F. K., Siebel, W., Wu, J. D., Zhu, X. Y., Shan, X. L., Sun, X. M. Late Mesozoic tectonic evolution of the Songliao basin, NE China: Evidence from detrital zircon ages and Sr–Nd isotopes. *Gondwana Res.*, 2012, **22**(3–4), 943–955.
26. Fildani, A., Hanson, A. D., Chen, Z. Z., Arriola, P. R. Geochemical characteristics of oil and source rocks and implications for petroleum systems, Talara basin, northwest Peru. *AAPG Bull.*, 2005, **89**(11), 1519–1545.
27. Espitalié, J., Marquis, F., Barsony, I. Geochemical logging. *Analytical Pyrolysis*, **184**, 276–304.
28. Langford, F. F., Blanc-Valleron, M. Interpreting Rock-Eval pyrolysis data using graphs of pyrolyzable hydrocarbons vs. total organic carbon. *AAPG Bulletin*, 1990, **74**(6), 799–804.
29. Bray, E. E., Evans, E. D. Distribution of *n*-paraffins as a clue to recognition of source beds. *Geochim. Cosmochim. Ac.*, 1961, **22**(1), 2–15.
30. Cranwell, P. A. Organic geochemistry of Cam Loch (Sutherland) sediments. *Chem. Geol.*, 1977, **20**, 205–221.

31. Ficken, K. J., Li, B., Swain, D. L., Eglinton, G. An *n*-alkane proxy for the sedimentary input of submerged/floating freshwater aquatic macrophytes. *Org. Geochem.*, 2000, **31**(7–8), 745–749.
32. Eglinton, G., Hamilton, R. J. Leaf epicuticular waxes. *Science*, 1967, **156**(3780), 1322–1335.
33. Didyk, B. M., Simoneit, B. R. T., Brassell, S. C., Eglinton, G. Organic geochemical indicators of palaeoenvironmental conditions of sedimentation. *Nature*, 1978, **272**(5650), 216–222.
34. Volkman, J. K., Maxwell, J. R. Acyclic isoprenoids as biological markers. In: *Biological Markers in the Sedimentary Record* (Johns, R. B., ed.). Elsevier, Amsterdam, 1986, 1–42.
35. Ten Haven, H. L., de Leeuw, J. W., Rullkötter, J., Sinninghe Damsté, J. S. Restricted utility of the pristane/phytane ratio as a palaeoenvironmental indicator. *Nature*, 1987, **330**(6149), 641–643.
36. Connan, J., Cassou, A. M. Properties of gases and petroleum liquids derived from terrestrial kerogen at various maturation levels. *Geochim. Cosmochim. Ac.*, 1980, **44**(1), 1–23.
37. Volkman, J. K., Barrett, S. M., Blackburn, S. I., Mansour, M. P., Sikes, E. L., Gelin, F. Microalgal biomarkers: A review of recent research developments. *Org. Geochem.*, 1998, **29**(5–7), 1163–1179.
38. Grantham, P. J., Wakefield, L. L. Variations in the sterane carbon number distributions of marine source rock derived crude oils through geological time. *Org. Geochem.*, 1988, **12**(1), 61–73.
39. Palmer, S. E. Hydrocarbon source potential of organic facies of the lacustrine Elko Formation (Eocene/Oligocene), northeast Nevada. In: *Hydrocarbon Source Rocks of the Greater Rocky Mountain Region* (Woodward, J., Meissner, F. F., Clayton, J. L., eds.). Rocky Mountain Association of Geologists, Denver, Colorado, 1984, 491–500.
40. Peters, K. E., Moldowan, J. M., Driscoll, A. R., Demaison, G. J. Origin of Beatrice oil by co-sourcing from Devonian and Middle Jurassic source rocks, inner Moray Firth, United Kingdom. *AAPG Bull.*, 1989, **73**(4), 454–471.
41. Peters, K. E., Snedden, J. W., Sulaeman, A., Sarg, J. F., Enrico, R. J. A new geochemical-sequence stratigraphic model for the Mahakam Delta and Makassar Slope, Kalimantan, Indonesia. *AAPG Bull.*, 2000, **84**(1), 12–44.
42. Hunt, J. M. *Petroleum Geochemistry and Geology*. Freeman and Company, 1996, 10–121.
43. Mackenzie, A. S., Brassell, S. C., Eglinton, G., Maxwell, J. R. Chemical fossils: the geological fate of steroids. *Science*, 1982, **217**(4559), 491–504.
44. Peters, K. E., Moldowan, J. M. *The Biomarker Guide: Interpreting Molecular Fossils in Petroleum and Ancient Sediments*. Prentice Hall, Englewood Cliffs, 1993.
45. Schoell, M., Hwang, R. J., Carlson, R. M. K., Welton, J. E. Carbon isotopic composition of individual biomarkers in gilsonites (Utah). *Org. Geochem.*, 1994, **21**(6–7), 673–683.
46. Grice, K., Schouten, S., Peters, K. E., Sinninghe Damsté, J. S. Molecular isotopic characterisation of hydrocarbon biomarkers in Palaeocene–Eocene evaporitic, lacustrine source rocks from the Jiangnan Basin, China. *Org. Geochem.*, 1998, **29**(5–7), 1745–1764.
47. Peters, K. E. Guidelines for evaluating petroleum source rock using programmed pyrolysis. *AAPG Bulletin*, 1986, **70**, 318–329.

48. Strobl, S. A. I., Sachsenhofer, R. F., Bechtel, A., Meng, Q. T., Sun, P. C. Deposition of coal and oil shale in NE China: The Eocene Huadian Basin compared to the coeval Fushun Basin. *Mar. Petrol. Geol.*, 2015, **64**, 347–362.

*Presented by S. Li*

Received November 30, 2017